J. Microbiol. Biotechnol. (2001), **11**(6), 1106–1110

JOURNAL OF
MICROBIOLOGY
AND
BIOTECHNOLOGY

Electron Microscopic Evidence of Parasporal Crystal Inclusion Biogenesis in *Bacillus sphaericus* Strain 1593

LEE, YOUNG JU AND HYUNG HOAN LEE*

Department of Biological Sciences, Konkuk University, Seoul 143-701, Korea

Received: May 10, 2001
Accepted: September 10, 2001

Abstract The parasporal biogenesis of crystal inclusion during the sporulation of *Bacillus sphaericus* strain 1593 was observed using transmission electron microscopy. The crystal biogenesis and sporulation process involved a sequence of events taking about 10 h. The sporulation processes were found to be similar to previous findings. The crystal biogenesis of *B. sphaericus* was initiated at the start of engulfment and nearly completed by the time of exosporium formation. The crystal formation was clearly associated with the outer forespore membrane from stages III through VI, and the crystals grew from polypeptide-like chains originated from the outer forespore membrane. These observations are different from previous findings, which report no association with the forespore membrane. The crystals were located adjacent to the outer membrane of the spore until the release stage. The axes size of the bipyramidal crystal was approximately 0.25 μm×0.42 μm. During crystal biogenesis, the crystal development could be classified into four stages; initiation stage C1 (sporulation stage III), growth stage C2 (sporulation III to V), envelopment and maturation C3 (sporulation V to VI), and finally release stage C4 (sporulation VII).

Key words: *Bacillus sphaericus*, endotoxin crystal, sporulation, forespore, electron microscopy

Bacillus sphaericus with larvicidal activity against several mosquito species was first reported by Kellen *et al.* [21]. The strains of *B. sphaericus* exhibit various spectra of activity toward larvae of three major genera of mosquitoes, *Culex*, *Anopheles*, and *Aedes* [1, 34]. The mosquito pathogeneses of *B. sphaericus* SSII-I [28, 30, 34], *B. sphaericus* 1593 [5, 7, 12, 23, 24, 29, 30, 32], *B. sphaericus* strain 2362 [12, 20], and *B. sphaericus* strain 2297 [6, 37] have already been extensively investigated and found to include insecticidal activity mediated through a proteinaceous parasporal crystal. The larvicidal crystal is found in close proximity to the spore enclosed within the exosporium [36, 37], and the crystal formation and sporulation would appear to be associated processes [9, 19, 37]. The crystals of *B. sphaericus,* which are separated from the spores, are composed of toxic precursor proteins, 110 and 125 kDa [3, 7, 10], and the precursors are activated into approximately 40 kDa to 56 kDa during sporulation [2, 8, 13]. In addition, there have been several electron microscopic observations of crystal formations in *B. sphaericus* strains [5, 11, 13], however, the detailed continuity of the parasporal crystal development has not yet been observed. Accordingly, the current study undertook an electron microscopic visualization of the parasporal crystal inclusion biogenesis during the sporulation of *B. sphaericus* strain 1593. The initial crystal formation appeared at sporulation stage III, thereafter, the incipient crystals grew, enveloped, matured, and were then released from the outercoat of the spore into the cytoplasm of the cells. During the process of sporulation, the cell underwent a complete transformation, and the parasporal events of the crystal development during the sporulation of the *B. sphaericus* strain 1593 were studied using transmission electron microscopy.

B. sphaericus strain 1593 (D. H. Dean, Ohio State University, U.S.A.) was used in this study. The bacteria were grown in a nutrient broth (Gibco, Gaithersburg, MD, U.S.A.) for 24 h at 30°C, and 20 ml of the culture was transferred and cultured in a NYSM broth (nutrient broth 0.9%, yeast extract 0.05%, 0.05 mM $MnCl_2$, 0.07 mM $CaCl_2$, 1.0 mM $MgCl_2$) [37] for 2 days at 30°C with shaking at 150 rpm. Next, the cultured cells were heated at 80°C in a water bath for 30 min with slight shaking and then stored at 4°C as a spore stock [22].

Six milliliters of the spore stock solution of *B. sphaericus* was inoculated into 194 ml of the NYSM broth, which was adjusted to an optical density (O.D.) of 0.2 at 600 nm, and then cultured at 30°C for 17 h with shaking at 150 rpm. At

*Corresponding author
Phone: 82-2-450-3426; Fax: 82-2-450-452-9715;
E-mail: hhlee@kkucc.konkuk.ac.kr

one-hour intervals, 10 ml of the culture was sampled, the growth of the cells measured at 600 nm, and the sample cultures were pelleted at 3,000 ×g for 30 min. The supernatants were discarded and the pellets were fixed in a 2% glutaraldehyde buffer.

Transmission electron microscopic visualization was carried out using the modified procedure described by Lee and Miller [26], Lee *et al.* [27], and Oh and Lee [31]. The samples were fixed in 2 ml of 2% glutaraldehyde in a 0.1 M phosphate buffer (pH 7.5) at room temperature for 1 h and then postfixed in 1% osmium tetroxide for another 2 h at 4°C. The samples were dehydrated, embedded, and sectioned. Finally, thin sections were examined using a Hitachi H-5000 transmission electron microscope at an accelerating voltage of 75 kV, and micrographs were made with Agfapan ISO100 film.

The morphological changes occurring during sporulation in the genera *Bacillus* have already been observed using electron microscopy and are conventionally subdivided into seven stages, I-VII [4, 15]. The spores of *B. sphaericus* 1593 were grown in the NYSM medium, and then sampled cells were measured by a spectrophotometer at an optical density of 0.2 at 600 nm every hour. The beginning of the stationary phase of the cell growth started 7 h post-culture (p.c.), and this time point was determined as the starting time of sporulation stage I. Thin sections of the samples were prepared to determine the crystal development in the cells during each sporulation stage, and the sequences of spore development and parasporal crystal biogenesis in the cells are shown in Figs. 1 to 6.

Sporulation: Certain sporogenic events and the biogenesis of crystal formation were found to be unique to *B. sphaericus* strain 1593, although the overall pattern of sporulation in the bacteria was similar to that of other bacilli [16, 17]. The sequence of spore development and biogenesis of parasporal crystal development in the bacteria is summarized in Table 1. In sporulation stage I (7 h), the formation of an axial chromatin filament took place. This observation is consistent with other reports [4, 5, 10, 17, 37]. In sporulation stage II (7 to 8 h), the subpolar forespore septum was formed by an invagination of the cell membrane near one of the ends of the cells, and the chromatin filament was separated into two chromosomes. The synthesis of the primary peptidoglycan layers between

Table 1. Sporulation and crystal biogenesis stages of *B. sphaericus* 1593.

	Events at culture hours									
Culture hours	7	8	9	10	11	12	13	14	15	17
Sporulation stages	I	II	III	III	IV	IV	V	V	VI	VII
Crystal biogenesis stages			C1	C2	C2	C2	C2	C3	C3	C4

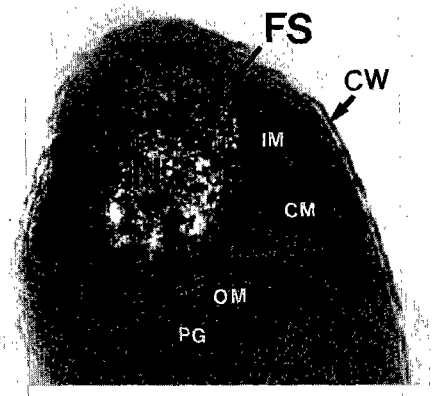

Fig. 1. Formation of the transverse cell wall during sporulation and first appearance of the crystalline protein matrix (CM) during engulfment of the forespore septum in sporulation stage III (9–10 h).

The crystalline proteins were attached to the outer forespore membrane on only one side. CW, cell wall; FS, forespore; IM, inner forespore membrane; OM, outer forespore membrane; N, nucleoid; PG, peptidoglycan layer. The size of the crystal matrix was 0.2 μm×0.13 μm. Bar indicates 0.4 μm.

two inner and outer membranes of the developing spore was observed. This gave rise to a septum separating the forespore and the mother cell, each containing a complete chromosome at the end of stage II (data not shown). In sporulation stage II, no crystal inclusion was visible. These results are consistent with other reports [4, 37]. In sporulation stage III (9 to 10 h), the forespore and mother cell protoplasts synthesized the peptidoglycan between the two inner and outer membranes of the developing spore (Fig. 1). Accordingly, at the end of stage III, the forespore was enclosed by two membranes. This stage was morphologically characterized by the engulfment of the septum, the formation of a free forespore, and primary crystal formation. The timing of the appearance of the primary crystal is consistent with findings in *B. sphaericus* strain 2297 [37] and in *B. thuringiensis* [4, 37]. It was observed that the crystalline matrix was parallel, in close contact with the outer membrane, and produced from the membrane concomitantly with the formation of the spore membrane at one area. Yousten and Davidson [37] and Bechtel and Bulla [4] also found such phenomenon in *B. thuringiensis*, where the primary crystal was biosynthesized at the opposite end of the spore [4]. Bechtel and Bulla [4] described an additional ovoid inclusion matrix without a crystalline structure in the variety *kurstaki*.

In sporulation stage IV (11 to 12 h), the primordial cell wall and spore cortex were established between the inner and outer membranes (Fig. 2). In sporulation stage V (13 to 14 h), the formation of the layers of the spore coat became evident (Fig. 3). In sporulation stage VI (15 h), the completion of the exosporium and the maturation of spores were witnessed (Figs. 4 and 5). In sporulation stage VII (16 h), the spores matured, however, they were not yet

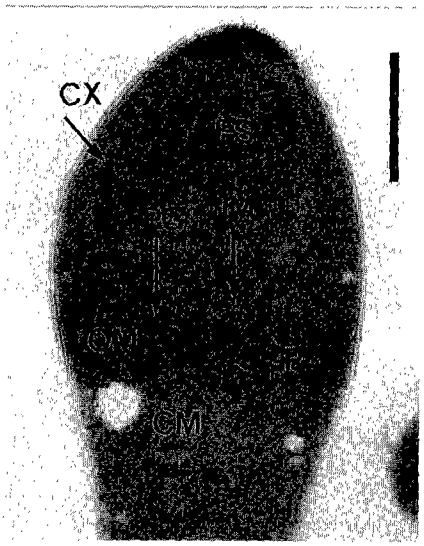

Fig. 2. Growing crystal and spore in sporulation stage IV (11–12 h).
The spore cortex (CX) and forespore (FS) are formed, surrounded by inner (IM) and outer (OM) membranes. The crystalline protein matrix (CM) is apart from the OM at a distance of 0.1 to 0.14 μm, yet linked to the outer membrane by a long polypeptide-like chain (P) derived from the OM. Bar, 0.36 μm.

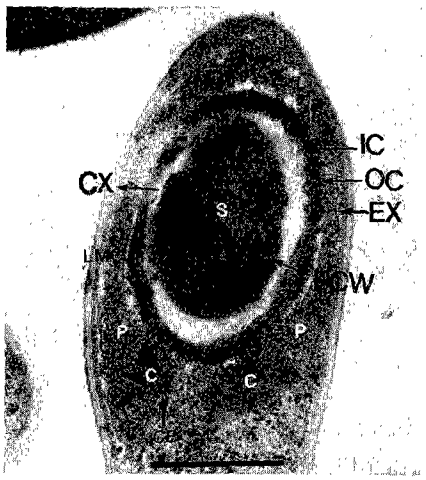

Fig. 4. Transverse section of sporulating cells in sporulation stage VI (15 h).
The matured and striated crystals (C) are hanging on the spore outer membrane (OC) by polypeptide chains (P) derived from the spore outer coat. Also, the crystals are partially enveloped (CE). The exosporium (EX) surrounding the spore (S) is completed. IC, spore inner coat; LMC, lamellar midcoat; PCW, primordial cell wall. Bar is 0.2 μm.

released from the cells (data not shown). Overall, the sporulation stages were generally found to be similar to other bacilli [14, 16, 17], however, *B. sphaericus* strain 1593 was unique in several points.

Crystal Biogenesis: The crystal development stages were arbitrarily divided into four stages based on electron microphotographic observation; C1 (8 to 9 h) – initiation stage of primary crystal formation; C2 (10 to 13 h) – growth stage of primary proteinaceous crystal matrix; C3 (14 to 15 h) – enveloping and maturation stage of crystal; and C4 – (17 h) detaching (release) stage of crystals from the spores into the cytoplasm. In the initiation stage C1, the crystal formation was initiated after 8 to 9 h of culture and the primary crystal matrix appeared in sporulation stage III (Fig. 1). The crystalline structure was tightly attached to

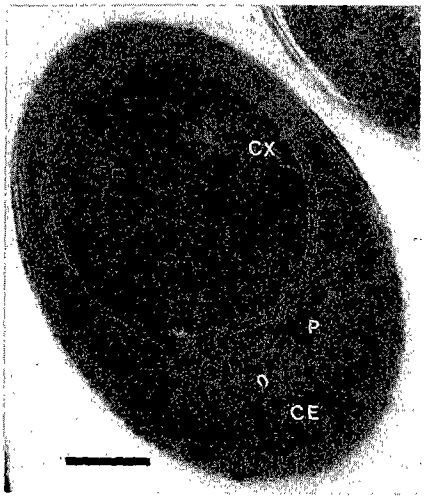

Fig. 3. Growing crystal and spore in sporulation stage V (13–14 h).
The primordial cell walls and cortex are formed. The crystalline protein matrix (CM) was linked to the outer membrane of the forespore by several polypeptide-like chains (P) derived from the OM, and partially enveloped (CE). Abbreviations are the same as for Fig. 2. Bar, 0.3 μm.

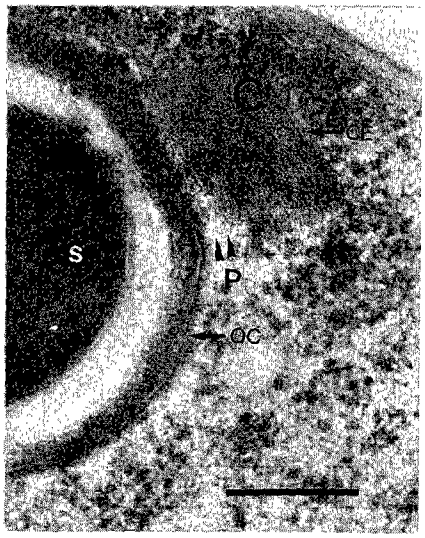

Fig. 5. Matured crystal (C) and spore (S) in longitudinal section in sporulation stage VI (15 h).
The matured crystals are enveloped (CE), connected to the outer spore membrane (OC) by polypeptide-like chains (P), and regularly striated. Bar, 0.2 μm.

the outer spore membrane and striated. The formation of the crystalline proteinaceous matrix was observed during engulfment in sporulation stage III, thereafter, the crystalline polypeptide subunits were progressively stacked and a matured bipyramidal crystal was finally produced in stage VI.

In the crystal growing stage C2 (sporulation III to V), the primary crystalline protein structure (CM) grew adjacent to the outer membrane of the forespore. One side of the crystalline proteins was attached to the outer membrane with several polypeptide-like chains derived from the outer membrane (Fig. 2). The crystal matrixes (CM) were detached and strung from the outer membrane. This would seem to indicate that the crystalline polypeptides were produced from the outer membrane, stacked, and then grew onto the crystalline main matrix. Using electron microscopy, Labaw [25] found that parasporal inclusions are constituted with a regular fine structure, thereby suggesting that the crystals are composed of subunits. The molecular weight of these subunits has been estimated at 230 kDa [18]. Yousten and Davidson [37] and Bechtel and Bull [4] also observed crystals attached to the outer membrane at this stage, however, they did not observe any growth of polypeptide-like chains derived from the outer forespore membrane.

In the crystal enveloping and maturation stage C3 (sporulation stages V and VI), the fluffy crystalline matrixes were mainly attached to the outer membrane of the forespore and also connected with several polypeptide-like chains (P) derived from the outer membrane (Fig. 3). The crystalline matrix, as shown in Fig. 3, was surrounded by rough edges, however, an envelope-like structure formed underneath the crystal.

As shown in Fig. 4, *B. sphaericus* produced more than one crystal in a cell, one triangular (0.15 μm underline and 0.15 μm height) and the other a right-angled tetragon (0.29 μm×0.12 μm). The two matured crystals remained connected to the outer coat of the mature spore by polypeptide-like chains, and the shape of the matured crystal had sharp edges without fuzzy materials during the formation of the spore coat layers and the completion of the exosporium surrounding the spore. Huber and Luthy [18] reported that each parasporal crystal inclusion body, surrounded by an envelope, consists of partially crystalline and amorphous material, while the shape of the inclusions provides stable characteristics. All crystals were located near or attached to the outer spore coats and the crystal matrix proteins were regularly arrayed and formed lattice structures with envelopes (Figs. 4 and 5). These indicate that the biogenesis of the crystalline proteins was closely linked to sporulation. Meanwhile, the parasporal inclusions revealed regular fine structure, suggesting that the crystals were composed of subunits. Short *et al.* [33] detected crystal antigens in the spore coat and exosporium. This fine structure is consistent with the reports by Yousten and Davidson [37] and de Barjac *et al.* [13]. In the crystal stage C4 (sporulation VII), the matured crystals and spores were separated within the cells (data not shown). In this stage, the cells containing spores and crystals were not lyzed. In the separation stage C4, the parasporal crystal exhibited a regular fine bipyramidal structure and was enveloped, suggesting that the crystals were composed of subunits, and the interior showed a crystalline lattice structure with striations. Finally, the dimensions of the matured bipyramidal crystal in the cell were approximately 0.25 μm×0.42 μm (data not shown), whereas the average axes size of a *B. thuringiensis* crystal is 0.8×2.0 μm [18].

During the sporulation process in *B. sphaericus* strain 1593, the cells underwent a complete transformation and the developmental events showing the growth of a parasporal crystal that was connected with certain polypeptide-like chains derived from the outer coat of the spore were observed using transmission electron microscopy. The crystal was formed during engulfment and was almost complete by the end of sporulation. The exosporium was formed during sporulation stage V, therefore, it was not involved in the formation of the crystals. The crystal was synthesized on the outer forespore membrane during sporulation stages III to VI, as demonstrated by serial section and numerous high-magnification micrographs. Accordingly, it is concluded that the parasporal crystal of *B. sphaericus* strain 1593 developed in four steps; initiation stage C1 (sporulation stages II to III), growth stage C2 (stages III to V), envelopment and maturation stage C3 (stage V to VI), and finally release stage C4 (stage VII).

Acknowledgments

This research was supported by a grant from Konkuk University, Seoul, Korea. The authors would like to thank the staff of the electron microscope laboratory at Yonsei University Hospital, Seoul, Korea for their technical assistance.

REFERENCES

1. Alexander, B. and F. G. Priest. 1990. Numerical classification and identification of *Bacillus sphaericus* including some strains pathogenic for mosquito larvae. *J. Gen. Microbiol.* **136:** 367–376.
2. Baumann, P., M. A. Clock, L. Baumann, and A. H. Broadwell. 1991. *Bacillus sphaericus* as a mosquito pathogen: Properties of the organism and its toxins. *Microbiol. Rev.* **55:** 425–436.
3. Baumann, P., B. M. Unterman, L. Baumann, A. H. Broadwell, S. J. Abbene, and R. D. Bowditch. 1985. Purification of the larvicidal toxin of *Bacillus sphaericus* and evidence for high-molecular-weight precursors. *J. Bacteriol.* **163:** 738–747.
4. Bechtel, D. B. and L. A. Bulla, Jr. 1976. Electron microscopic study of sporulation and parasporal crystal formation in *Bacillus thuringiensis*. *J. Bacteriol.* **127:** 1472–1481.

5. Bourgouin, C. and J. F. Charles. 1981. Ultrastructure des spores de *Bacillus sphaericus* apres extraction physigue D'un facteur toxique pour les larves d'Anopheles. *Rev. Cytol. Biol. Veg. Bot.* **4:** 99–109.
6. Bourgouin, C., J.-F. Charles, A. R. Kalfon, and H. de Barjac. 1984. *Bacillus sphaericus* 2297. Purification and biogenesis of parasporal inclusions, toxic for mosquito larvae. pp. 389–390. *In* J. E. Alouf, F. J. Fehrenbach, J. F. Freer, and J. Jeljaszewicz (eds.), *Bacterial Protein Toxins.* Academic Press, Inc. (London), Ltd., London, U.K.
7. Bourgouin, C., R. Tinelli, J.-P. Bouvet, and R. Pires. 1984. *Bacillus sphaericus* 1593-4. Purification of fractions toxic for mosquito larvae, pp. 387–388. *In* J. E. Alouf, F. J. Fehrenbach, J. F. Freer, and J. Jeljaszewicz (eds.), *Bacterial Protein Toxins.* Academic Press, Inc., London, U.K.
8. Broadwell, A. H., L. Bauman, and P. Bauman. 1990. The 42- and 51-kilodalton mosquitocidal proteins of *Bacillus sphaericus* 2362: Construction of recombinants with enhanced expression and *in vivo* studies of processing and toxicity. *J. Bacteriol.* **172:** 2217–2223.
9. Broadwell, A. H. and P. Bauman. 1987. Sporulation-associated activation of *Bacillus sphaericus* larvicide. *Appl. Environ. Microbiol.* **52:** 758–764.
10. Charles, J.-F., A. Kalfon, C. Bourgouin, and H. de Barjac. 1988. *Bacillus sphaericus* asporogenous mutants: Morphology, protein pattern and larvicidal activity. *Ann. Inst. Pasteur/ Microbiol.* **139:** 243–259.
11. Davidson, E. W. and P. Myers. 1981. Parasporal inclusions in *Bacillus sphaericus. FEMS Microbiol. Lett.* **10:** 261–265.
12. Davidson, E. W., M. Urbina, J. Payne, M. S. Mulla, H. Darwazeh, H. T. Dulmage, and J. A. Correa. 1984. Fate of *Bacillus sphaericus* 1593 and 2362 spores used as larvicides in the aquatic environment. *Appl. Environ. Microbiol.* **47:** 125–129.
13. de Barjac, H., I. Thiery, V. Cosmao-Dumanoir, E. Frachon, P. Laurent, J.-F. Charles, S. Hamon, and J. Ofori. 1988. Another *Bacillus sphaericus* serotype harboring strains very toxic to mosquito larvae: Serotype H6. *Ann. Inst. Pasteur/ Microbiol.* **139:** 363–377.
14. Decker, S. and S, Maier. 1975. Fine structure of mesosomeal involvement during *Bacillus sphaericus* sporulation. *J. Bacteriol.* **121:** 363–372.
15. Dworkin, M. 1985. *Developmental Biology of the Bacteria.* pp. 22–31. Benjamin/Cummings Publishing Co., Menlo, California, U.S.A.
16. Ellar, D. J. and D. G. Lundgren. 1966. Fine structure of sporulation in *Bacillus cereus* grown in chemically defined medium. *J. Bacteriol.* **92:** 1748–1764.
17. Holt, S. C., J. J. Gauthier, and D. J. Tipper. 1975. Ultrastructural studies of sporulation in *Bacillus sphaericus. J. Bacteriol.* **122:** 1322–1338.
18. Huber, H. and P. Luthy. 1981. *Bacillus thuringiensis* delta endotoxin:composition and activation. pp. 207–234. *In* E. W. Davidson (ed.), *Pathogenesis of Invertebrate Microbial Disease.* Allanheld, Osmun and Co., Totowa, N.J., U.S.A.
19. Kalfon, A., J. F. Charles, C. Bourgouin, and H. de Barjac. 1984. Sporulation of *Bacillus sphaericus* 2297: An electron microscope study of crystal-like inclusion biogenesis and toxicity to mosquito larvae. *J. Gen. Microbiol.* **130:** 893–900.
20. Karch, S. and J.-F. Charles. 1987. Toxicity, viability and ultrastructure of *Bacillus sphaericus* 2362 spore/crystal complex used in the field. *Ann. Inst. Pasteur/Microbiol.* **138:** 458–492.
21. Kellen, W. R., T. B. Clark, J. E. Lindegren, B. C. Ho, M. H. Rogoff, and S. Singer. 1965. *Bacillus sphaericus* Neide as a pathogen of mosquitoes. *J. Invertebr. Pathol.* **7:** 442–448.
22. Kim, S. Y., M. H. Kang, H. B. Choi, J. U. Lee, J.-F. Charles, V. C. Dumanoir, M.-M. Lecadet, and H. H. Lee. 1999. Characteristics of thirty-six *Bacillus thuringiensis* isolates and a new serovar. of *Bacillus thuringiensis* subsp. Kim (serotype H52). *J. Microbiol. Biotechnol.* **9:** 534–540.
23. Kim, Y. H. and H. H. Lee. 1984. Isolation of sporeless temperature-sensitive mutants of *Bacillus sphaericus. Han Guk J. Genetic Eng.* **1:** 15–21.
24. Kim, Y. H. and H. H. Lee. 1985. Isolation of conditional lethal temperature-sensitive mutants of *Bacillus sphaericus. Kor. J. Appl. Microbiol. Bioeng.* **13:** 41–49.
25. Labaw, L. W. 1964. The structure of *Bacillus thuringiensis* Berliner crystals. *J. Ultrastruct. Res.* **10:** 66–75.
26. Lee, H. H. and L. K. Miller. 1979. Isolation and initial characterization of temperature-sensitive mutants of *Autographa californica* nuclear polyhedrosis virus. *J. Virol.* **31:** 240–252.
27. Lee, W.-W., B.-J. Lee, Y. Lee, Y.-S. Lee, and J.-H. Park. 2000. *In situ* hybridization of white spot disease virus in experimentally infected penaeid shrimp. *J. Microbiol. Biotechnol.* **10:** 215–220.
28. Myers, P. and A. A. Yousten. 1979. Localization of a mosquito-larval toxin of *Bacillus sphaericus* SSII-I for mosquito larvae. *Infect. Immunity* **19:** 1047–1053.
29. Myers, P. and A. A. Yousten. 1980. Localization of a mosquito-larval toxin of *Bacillus sphaericus* 1593. *Appl. Environ. Microbiol.* **39:** 1205–1211.
30. Myers, P., A. A. Yousten, and E. W. Davidson. 1979. Comparative studies of the mosquito-larval toxin of *Bacillus sphaericus* SSII-I and 1593. *Can. J. Microbiol.* **25:** 1227–1231.
31. Oh, C. K. and H. H. Lee. 1987. Electron microscope studies of infection and multiplication of *Autographa californica* nuclear polyhedrosis virus clone L-1 and ts-B1074. 1. Infection and multiplication of *A. californica* NPV L-1. *J. Kor. Soc. Virol.* **17:** 61–72.
32. Payne, J. M. and E. W. Davidson. 1984. Insecticidal activity of the crystalline parasporal inclusions and other components of *Bacillus sphaericus* 1593 spore complex. *J. Invertebr. Pathol.* **43:** 383–388.
33. Short, J. A., P. D. Walker, R. O. Thomson, and H. J. Somerville. 1974. The fine structure of *Bacillus thuringiensis* spores with special reference to the location of crystal antigen. *J. Gen. Microbiol.* **84:** 261–276.
34. Singer, S. 1974. Entomogenous bacilli against mosquitos larvae. *Dev. Ind. Microbiol.* **15:** 187–194.
35. Somerville, H. J. 1971. Formation of the parasporal inclusion of *Bacillus thuringiensis. Eur. J. Biochem.* **18:** 226–237.
36. Yousten, A. A. 1984. *Bacillus sphaericus*: Microbiological factors related to its potential as a mosquito larvicide. *Adv. Biotechnol. Processes* **3:** 315–343.
37. Yousten, A. A. and E. Davidson. 1982. Ultrastructural analysis of spores and parasporal crystal formed by *Bacillus sphaericus* 2297. *Appl. Environ. Microbiol.* **446:** 1449–1455.